Cell Reports

Resource

Genome-wide RNAi Screen Identifies Cohesin Genes as Modifiers of Renewal and Differentiation in Human HSCs

Graphical Abstract

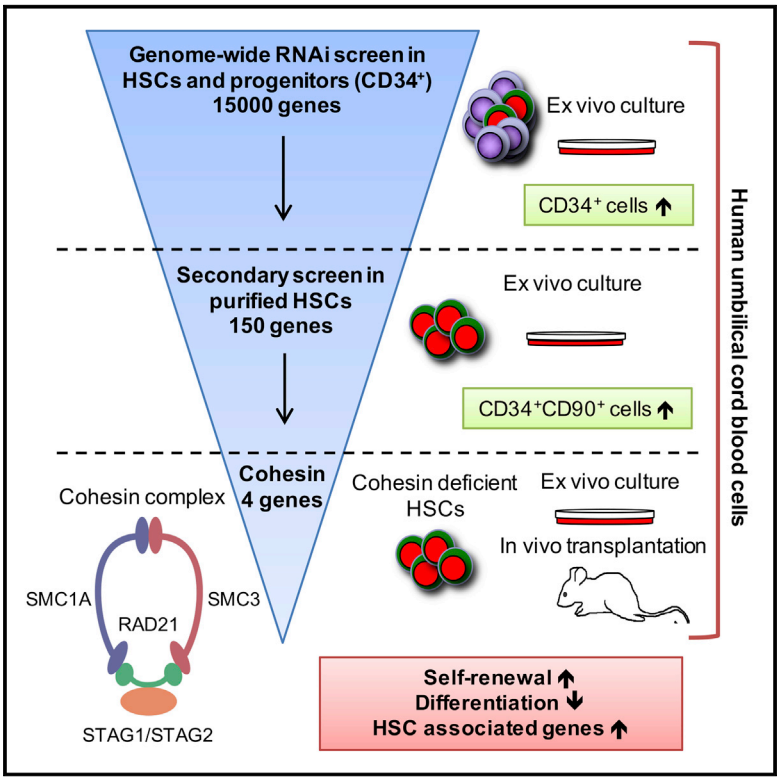

Authors

Roman Galeev, Aurélie Baudet, Praveen Kumar, ..., Åke Borg, Anders Kvist, Jonas Larsson

Correspondence

jonas.larsson@med.lu.se

In Brief

Galeev et al. report on a genome-wide RNAi screen targeted to primary human hematopoietic stem and progenitor cells. They identify several members of the cohesin complex as critical modifiers of renewal and differentiation. Cohesin deficiency induces HSC-specific gene programs and triggers an expansion phenotype in vitro and in vivo.

Highlights

- A genome-wide RNAi screen was performed in primary human CD34+ cells
- Several cohesin genes were identified as modifiers of renewal and differentiation
- Cohesin-deficient HSCs show enhanced reconstitution capacity in vivo
- Cohesin deficiency induces immediate HSC-specific transcriptional programs

Accession Numbers

GSE74824

Galeev et al., 2016, Cell Reports *14*, 2988–3000
March 29, 2016
http://dx.doi.org/10.1016/j.celrep.2016.02.082

OPEN ACCESS
CellPress

Cell Reports
Resource

Genome-wide RNAi Screen Identifies Cohesin Genes as Modifiers of Renewal and Differentiation in Human HSCs

Roman Galeev,[1] Aurélie Baudet,[1] Praveen Kumar,[1] Alexandra Rundberg Nilsson,[2] Björn Nilsson,[4] Shamit Soneji,[2] Therese Törngren,[3] Åke Borg,[3] Anders Kvist,[3] and Jonas Larsson[1,*]
[1]Division of Molecular Medicine and Gene Therapy, Lund Stem Cell Center, Lund University, 221 84 Lund, Sweden
[2]Division of Molecular Hematology, Lund Stem Cell Center, Lund University, 221 84 Lund, Sweden
[3]Division of Oncology and Pathology, Lund University, 223 63 Lund, Sweden
[4]Division of Hematology and Transfusion Medicine, Lund University, 221 84 Lund, Sweden
*Correspondence: jonas.larsson@med.lu.se
http://dx.doi.org/10.1016/j.celrep.2016.02.082

SUMMARY

To gain insights into the regulatory mechanisms of hematopoietic stem cells (HSCs), we employed a genome-wide RNAi screen in human cord-blood derived cells and identified candidate genes whose knockdown maintained the HSC phenotype during culture. A striking finding was the identification of members of the cohesin complex (*STAG2*, *RAD21*, *STAG1*, and *SMC3*) among the top 20 genes from the screen. Upon individual validation of these cohesin genes, we found that their knockdown led to an immediate expansion of cells with an HSC phenotype in vitro. A similar expansion was observed in vivo following transplantation to immunodeficient mice. Transcriptome analysis of cohesin-deficient $CD34^+$ cells showed an upregulation of HSC-specific genes, demonstrating an immediate shift toward a more stem-cell-like gene expression signature upon cohesin deficiency. Our findings implicate cohesin as a major regulator of HSCs and illustrate the power of global RNAi screens to identify modifiers of cell fate.

INTRODUCTION

Human hematopoiesis is maintained by a small number of hematopoietic stem cells (HSCs) that are capable of generating all blood cell lineages at an extremely rapid pace for the entire lifespan of a human being (Orkin and Zon, 2008). HSCs have been studied extensively during the last four decades and are probably the best functionally characterized adult stem cells. However, despite this, the regulatory mechanisms that govern different cellular fate options in HSCs have remained incompletely defined. In particular, it has been challenging to understand the molecular basis of the inherent ability of HSCs to self-renew and preserve their undifferentiated state, which has hampered efforts to expand HSCs ex vivo for therapeutic benefit (Dahlberg et al., 2011). Ex vivo expansion of HSCs would allow for critical improvements of bone marrow transplantation procedures in treatment of malignant and inherited hematological diseases (Chou et al., 2010). Defining the genetic and molecular basis of self-renewal of HSCs is thus important to enhance current cell-therapy strategies, but it is also essential in order to better understand mechanisms behind dysregulated hematopoiesis that may cause leukemia. Genes and pathways balancing cell-fate options between renewal and differentiation in stem cells are often key players in cancer development (Orkin and Zon, 2008).

Traditionally, assessment of gene function in mammals has been based on reverse genetic approaches in which individual candidate genes are studied. However, the development of RNAi technology about a decade ago has transformed functional genetics and provided tools to perform forward genetic screens in primary mammalian cells (Hannon and Rossi, 2004). RNAi screening has emerged as a powerful tool to genetically dissect functional aspects of both normal and malignant HSCs using short hairpin RNA (shRNA) retroviral and lentiviral vector-libraries (Karlsson et al., 2014). Recent studies have identified fate determinants in murine HSCs through focused screens targeting histone modifiers (Cellot et al., 2013), polycomb repressor complex (PRC) genes (Kinkel et al., 2015), and regulators of polarity and asymmetric cell division (Hope et al., 2010). RNAi screens have also successfully identified several important driver genes in malignant hematopoiesis, most notably in acute myeloid leukemia, both in vitro (Zuber et al., 2011) and in vivo (Miller et al., 2013). These studies have also been performed in murine settings using pre-selected libraries targeting specific gene categories or families.

Our laboratory has developed paradigms to perform forward RNAi screens in primary human hematopoietic stem and progenitor cells (HSPCs), using pooled lentiviral shRNA libraries (Ali et al., 2009; Baudet et al., 2012). From a screen targeting mainly kinases and phosphatases, we reported the identification of MAPK14 (p38) as a druggable modifier of expansion of umbilical cord blood (CB)-derived HSPCs, supporting the feasibility of RNAi screens as a tool for gene discovery in primary human hematopoietic cells (Baudet et al., 2012). However, these previous screens have been limited to around 1,000 genes and have not

directly assessed stem cell properties. Here, we now report on the development of a two-step screening paradigm to address these limitations. We first targeted a near genome-wide lentiviral shRNA library to human CB-derived $CD34^+$ cells to globally define genes restricting expansion of HSPCs. The highest ranked genes were subsequently subjected to a secondary screen in highly purified HSCs to filter out stem-cell-specific outcomes related to self-renewal and differentiation. From this approach, we have discovered putative regulators of cell fate in HSCs and specifically identified several components of the cohesin complex as critical regulators of HSC renewal and differentiation both in vitro and in vivo.

RESULTS

Genome-wide RNAi Screen in Primitive Human Hematopoietic Cells Defines Genes and Pathways Associated with Cell Expansion and Cancer Development

In order to globally search for modifiers of HSC renewal and differentiation, we performed a near genome-wide, pooled lentiviral shRNA screen in primary human CB-derived $CD34^+$ cells. As a basis for the screen, we used the limited persistence of the immature cell phenotype ($CD34^+$) under ex vivo culture conditions, selecting for shRNAs conferring increased expansion of stem and progenitor cells. We have previously shown using smaller libraries that this approach enables the identification of genes and pathways that influence renewal and differentiation of HSCs (Ali et al., 2009; Baudet et al., 2012).

We used a lentiviral library consisting of 75,000 shRNA vectors targeting 15,000 genes developed by the RNAi Consortium (TRC) at the Broad Institute and distributed as pooled lentiviral particles by Sigma Aldrich (Figure S1A). To ensure optimal representation of the highly complex library in the screen, we collected $CD34^+$ cells from more than 100 CB units. A total of 60 million $CD34^+$ cells were subsequently transduced with the library in six replicate screens (Figure 1A). To avoid multiple shRNA integrations in a single cell, we aimed to keep the transduction efficiency below 37% and validated this by clonal PCR analysis of vector integration in hematopoietic colonies from transduced the cells (Figure S1B). On average, the transduction efficiency was 30%.

Following transduction, the cells were cultured for 20 days in serum-free medium supplemented with growth factors. We assessed the distribution of all shRNAs in the library by next-generation sequencing of integrated proviruses amplified from genomic DNA of $CD34^+$ cells, 3 days after transduction and following 20 days of culture (Figure 1A). The change in the relative contribution the shRNAs over time was used to identify those influencing the expansion of $CD34^+$ cells. We thus determined the ratios between the normalized counts for all shRNAs between day 20 and day 3 and plotted them from the most enriched to the most depleted (Figure 1B). Out of the 75,000 shRNAs included in the library, we could readily detect 68,000 (91%) at both time points; the remaining shRNA were excluded from further analysis. The overall coverage of the library in the screen was consequently estimated to be 300X (i.e., each shRNA was targeted to on average 300 cells). As $CD34^+$ cells represent a relatively heterogeneous population of stem and progenitor cells, we reasoned that this level of coverage would be best suited for identification of phenotypes detected by positive selection through enrichment of shRNAs, rather than depletion phenotypes which typically require higher coverage and more uniform cells with coordinated behavior for accurate detection. Moreover, as depletion events in RNAi screens are more likely to be influenced by confounding effects from off-target activity on essential genes or general toxicity of certain shRNAs, we first focused our analysis on the enriched fractions of shRNAs and thus the identification of genes restricting HSPC expansion in the screening assay.

To test broadly whether the screen had selected for relevant outcomes with respect to cell expansion, we first performed a global analysis of all genes targeted by two or more shRNAs within the 10% most enriched fraction (Figure 1B). Gene ontology (GO) analysis of the resultant 1,023 genes (Table S1) showed, in line with our expectations, that the most enriched gene category was one for genes associated with negative regulation of cell proliferation (Figure 1C). Moreover, KEGG pathway analysis showed a strong enrichment for several cancer-associated genes and pathways (Figure 1D). Taken together, this illustrates a strong propensity of the unbiased near genome-wide screen to identify genes inhibiting cell proliferation, as well as genes involved in cancer development, and validates, in general terms, the feasibility of our approach as a tool to globally define genes that modify cell expansion in human HSPCs.

A Secondary Screen Targeted to $CD34^+CD38^-CD90^+CD45RA^-$ Cells Identifies the Cohesin Complex as a Candidate Regulator of HSC Renewal and Differentiation

Our genome-wide screen in $CD34^+$ cells had identified a large number of candidate genes as potential negative regulators of cell expansion. However, this first selection of genes was based on a relatively loose definition (two shRNAs among the 10% most enriched) and could be significantly influenced by noise from, e.g., random off-target activity from certain shRNAs. Moreover, CD34 marks a broad repertoire of both stem cells and progenitor cells and our primary screening assay did not distinguish between general effects on proliferation and an actual impact on stem cell self-renewal. Therefore, in order to further prioritize among the candidate genes and to filter out the most significant hits with a functional impact on bona fide HSCs, we decided to apply strict criteria to rank the genes and then to perform a secondary screen for the highest ranked genes in purified HSC populations using a more precise readout for stem cell activity.

To rank the genes, we first assigned a stringent value to each shRNA based on the level of enrichment and, when applicable, the documented knockdown efficiency (data available from Sigma Aldrich for approximately 50% of all shRNAs). A score was then calculated for each gene based on the accumulated values of the corresponding shRNAs and to what extent the gene was expressed in immature hematopoietic cells (for details, see the Supplemental Experimental Procedures). The final ranking based on this score for the top 1,000 genes is shown in Figure 2A, and the genes are listed in Table S2. The 150

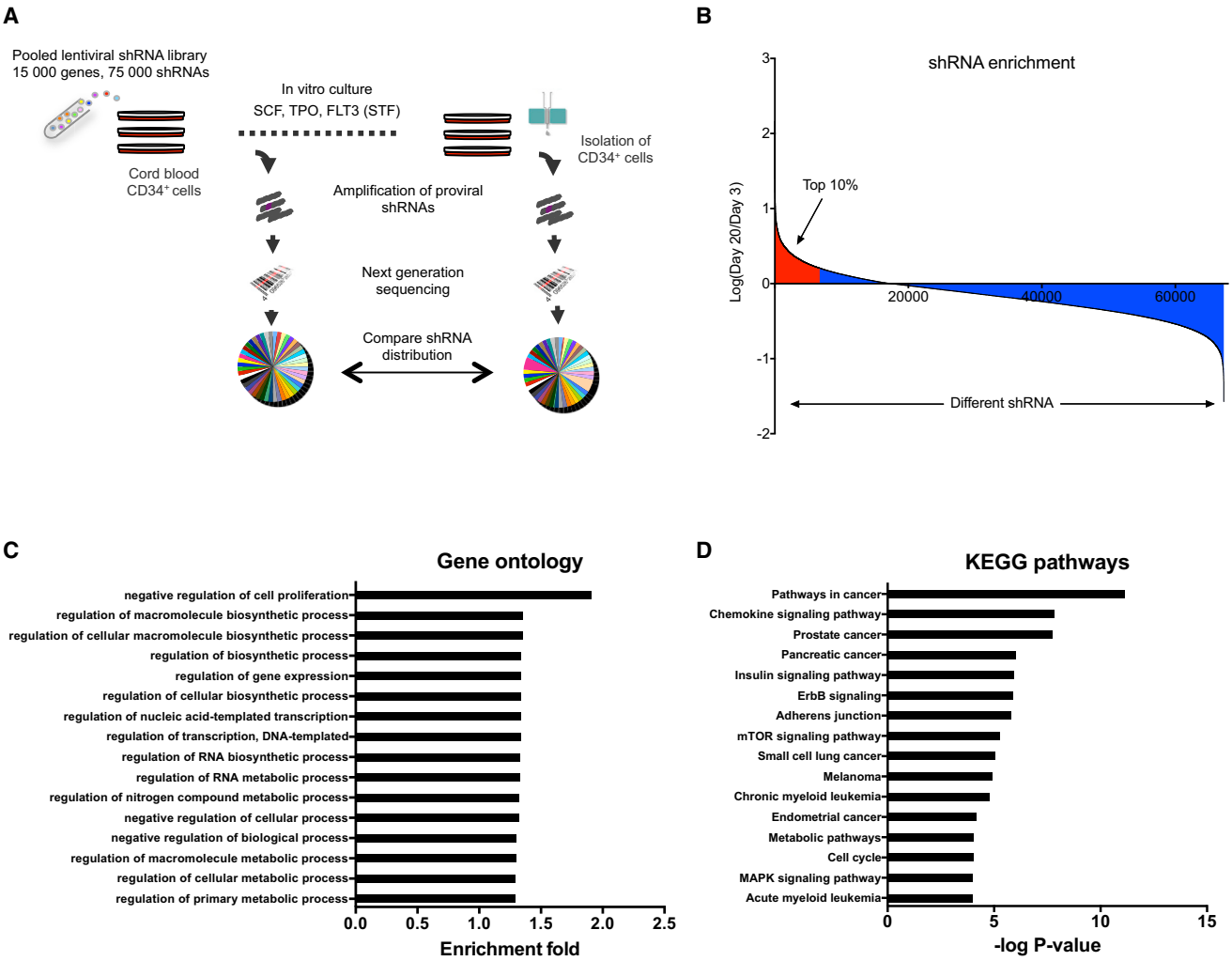

Figure 1. Genome-wide RNAi Screen in Primitive Human Hematopoietic Cells Defines Genes and Pathways Associated with Cancer Progression and Cell Proliferation

(A) Overview of the experimental outline for the primary screen. 60 million cord blood-derived $CD34^+$ cells were transduced with a pooled lentiviral library containing 75,000 shRNAs across six transduction replicates in total. A fraction of the cells were isolated after 72 hr, and proviral inserts were deep sequenced to determine the initial library distribution. Following 20 days of culture, $CD34^+$ cells were magnetically isolated and proviral inserts were sequenced again to determine the changes in distribution for all shRNAs.

(B) Relative distribution of shRNAs following 20 days of in vitro culture, ranked from the most enriched to the most depleted. The y axis shows the average enrichment value across six replicate screens.

(C) Gene ontology analysis for all genes represented by multiple shRNAs in the most enriched (10%) fraction.

(D) KEGG pathway analysis showing strong enrichment for cancer-associated pathways among the top-scoring genes.

See also Figure S1 and Table S1.

highest scoring genes were subsequently selected for the secondary screen and are marked in red in Figure 2A.

Next, we created a pooled shRNA library consisting of a total of 350 shRNAs against the 150 selected candidate genes. With this smaller library, we reasoned that it would be feasible to perform a robust screen in the discrete population of $CD34^+CD38^-CD90^+CD45RA^-$ cells that is highly enriched in bona fide HSCs (Majeti et al., 2007). When cultured ex vivo, the $CD34^+CD38^-CD90^+CD45RA^-$ cells show a strong propensity to differentiate and give rise to three distinct populations based on expression of CD34 and CD90 after several days; $CD34^+CD90^+$, $CD34^+CD90^-$, and $CD34^-CD90^-$. We have recently demonstrated that the in vivo long-term repopulation potential in such cultures is exclusively contained within the double-positive $CD34^+CD90^+$ cells, while the vast majority of committed progenitor cells are found in the $CD34^+CD90^-$ population (A.B. and J.L., unpublished data). Tracking of the $CD34^+CD90^+$ population is therefore a sensitive and specific tool to predict stem cell activity in cultured hematopoietic cells and provides an excellent basis for a screen aimed at detecting outcomes influencing self-renewal and differentiation of functional HSCs.

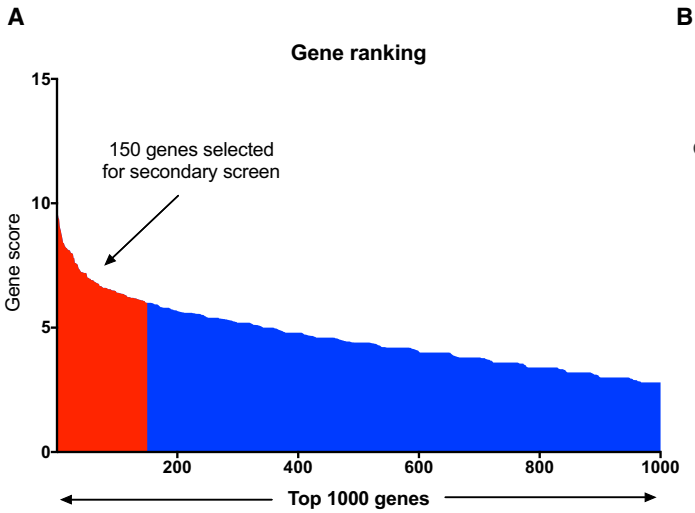

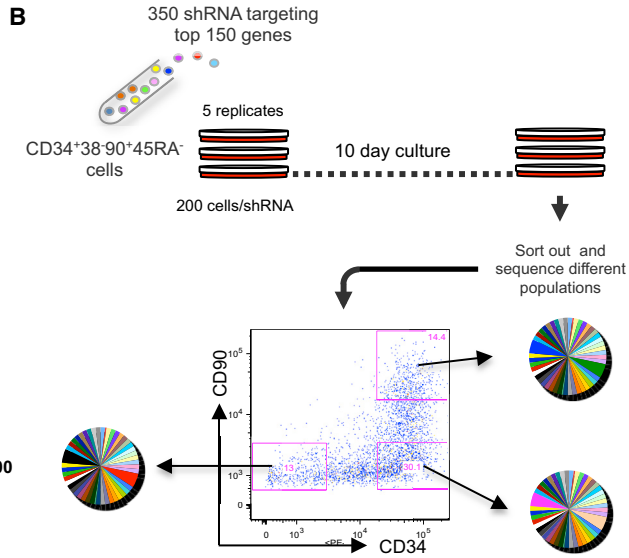

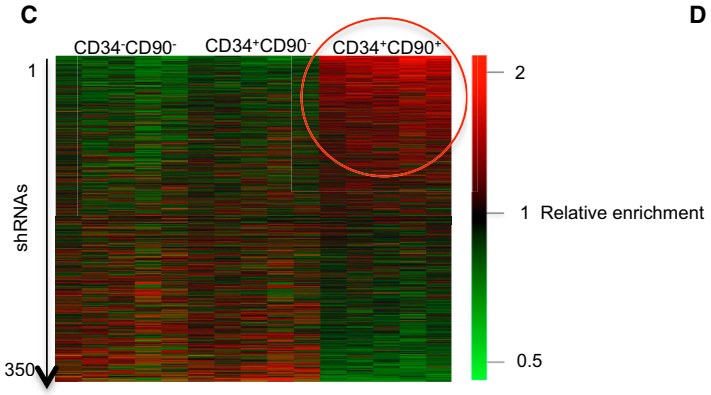

D

Gene rank	Gene	Gene score
1	RTCD1	49,03
2	STAG2	42,86
3	ADIPOR2	41,58
4	TACO1	39,28
5	PDPK1	39,15
6	SERPINA4	37,63
7	DUSP8	37,15
8	SYTL2	36,51
9	USP21	36,31
10	KRIT1	36,28
11	RAD21	35,98
12	C12orf43	35,65
13	DDX6	35,41
14	BRD7	35,31
15	SLC28A1	34,76
16	STAG1	34,68
17	SMC3	34,23
18	FLT3	34,07
19	KATNB1	33,80
20	PRR14	33,69
21	HIRA	33,69
22	TRAIP	33,49
23	ZNF573	33,40
24	MKRN2	33,18
25	ARRB1	33,13
26	FMR1	33,07
27	LTC4S	33,02
28	ATP5D	33,01
29	CDX2	32,83
30	LSS	32,75

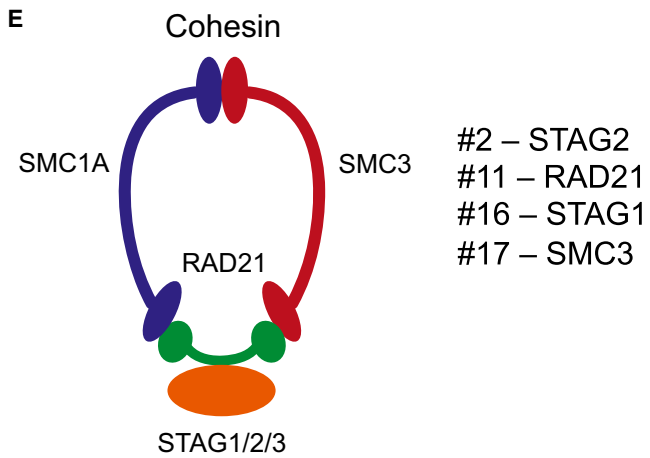

(legend on next page)

For the secondary screen, we sorted $CD34^+CD38^-CD90^+CD45RA^-$ cells from a total of 50 CB units and transduced with the pooled shRNA library (with a final coverage of on average 200 cells per shRNA). Following 10 days of in vitro culture, we sorted out the three distinct populations based on CD34 and CD90 expression (Figure 2B). The distribution of all shRNAs within these three populations was analyzed by deep sequencing of proviral inserts as described above. Comparison of the normalized sequencing counts between these three populations gave us the opportunity to determine how cells targeted by a given shRNA had been distributed between the three populations (Figure 2C). For all shRNAs in the library we could thus determine their influence on renewal and differentiation, independent of any effects on cell proliferation. Based on this, we ranked all shRNAs according to their ability to maintain the $CD34^+CD90^+$ population and defined the top-scoring genes as those having the highest enrichment of $CD34^+CD90^+$ cells across their corresponding shRNAs (Figure 2D; Table S3).

The most notable finding when analyzing the highest scoring genes from the secondary screen was the presence of several members of the cohesin complex. The cohesin complex consists of five subunits (STAG1, STAG2, RAD21, SMC1A, and SMC3) (Gruber et al., 2003; Nasmyth and Haering, 2009), and we identified no fewer than four of these (*STAG1*, *STAG2*, *RAD21*, and *SMC3*) among our top 20 genes, strongly pointing toward a crucial function of the cohesin complex in regulation of HSCs (Figure 2E). Moreover, recent large-scale sequencing studies have identified recurrent mutations in the cohesin genes in myeloid malignancies, also suggesting a functional role of these genes in hematopoiesis (Kon et al., 2013; Papaemmanuil et al., 2013; Welch et al., 2012). We therefore decided to focus our further analysis on these genes and determine in higher detail the functional role of the cohesin complex in human HSCs.

Knockdown of Cohesin Genes Restricts Differentiation and Expands Primitive Cells In Vitro

To investigate the role of cohesin in human hematopoiesis, we first analyzed the expression pattern of the four cohesin genes identified in our screen in subsets of hematopoietic cells ranging from HSCs to committed progenitors, as well as more differentiated cells (Figures S2A and S3A). Overall, we found that the cohesin genes were robustly and widely expressed across all these subsets and did not appear to be preferentially expressed in any of the populations (Figures S2B and S3B). STAG2 and RAD21 showed around 2-fold higher expression compared to STAG1 and SMC3 for most of the cell types.

Next, we assayed the knockdown efficiency of each shRNA vector targeting the cohesin genes. All the shRNAs that had been picked out of the screen-exhibited knockdown of their respective genes in human $CD34^+$ cells (Figure 3A), and the level of knockdown correlated well with the degree of enrichment exhibited in the screen (data not shown). We then functionally validated each lentiviral shRNA vector in individual experiments in $CD34^+$-sorted cells to ascertain whether the observed enrichment of the cohesin complex members was a true positive hit. For this purpose we used a vector expressing GFP (Figure S4A) to be able to track the transduced cells during culture. $CD34^+$-sorted cells were transduced with either a control (scrambled shRNA) vector or shRNAs targeting each of the cohesin genes (two shRNAs each for RAD21 and SMC3 and three shRNAs each for STAG1 and STAG2). The transduced cells were cultured in serum-free medium supplemented with growth factors and analyzed by flow cytometry every week during 4 weeks to determine the expression levels of CD34 and CD90 in the GFP-positive cells (Figure 3B). During the 4-week culture period, all shRNAs showed an increased expansion of both total $CD34^+$ cells (Figure S4B) and the HSC-enriched $CD34^+CD90^+$ population (Figures 3B and 3C) compared to controls. Knockdown of STAG2, in particular, showed a clear correlation between knockdown levels and expansion of the $CD34^+CD90^+$ population, but also knockdown of SMC3 and RAD21 displayed a dose-dependent phenotype. Taken together, this shows that reduced expression of cohesin genes preserves the immature state of human HSPCs in culture.

Cohesin-Deficient HSCs Show Delayed Differentiation but Overall Increased Reconstitution Potential following Transplantation to Primary and Secondary Immunodeficient Mice

Given the profound effects executed by cohesin knockdown in cultured human HSPCs, we next wanted to assess the role of cohesin in a physiological context in vivo. This would further allow us to more accurately evaluate any HSC-specific outcomes. Since STAG2 knockdown had shown the strongest effect on the $CD34^+CD90^+$ population across all three shRNAs and was the highest scoring cohesin gene from the screen, we decided to initially focus on this gene when evaluating effects of cohesin knockdown in vivo. Cord blood-derived $CD34^+CD38^-CD90^+CD45RA^-$ cells were transduced with lentiviral shRNA vectors (shSTAG2 and scrambled control), sorted for GFP expression shortly after transduction (36 hr), and transplanted into sublethally irradiated NOD.Cg-Prkdc^{scid}Il2rg^{tm1Wjl}/SzJ (NSG) mice (Figure 4A). When the mice were first analyzed for human

Figure 2. A Targeted Screen in Highly Enriched HSC Populations Identifies Cohesin Genes as Candidate Regulators of Renewal and Differentiation

(A) Ranking of the top genes from the primary screen. The highest scoring fraction of genes selected for the secondary screen is marked in red.

(B) Overview of the experimental outline for the targeted secondary shRNA screen. Cells highly enriched for human HSCs ($CD34^+38^-90^+45RA^-$ cells) were sorted and transduced with the pooled targeted library consisting of shRNAs for the highest scoring genes. After 10 days of culture, three different populations based on their CD34 and CD90 expression were sorted and subjected to sequencing to determine the shRNA distribution.

(C) Illustrative heatmap over the distribution for each shRNA across the three cell populations.

(D) Genes ranked based on their corresponding shRNAs' ability to maintain the $CD34^+CD90^+$ phenotype.

(E) Overview of the cohesin complex and the respective genes identified in the screen.

See also Tables S2 and S3.

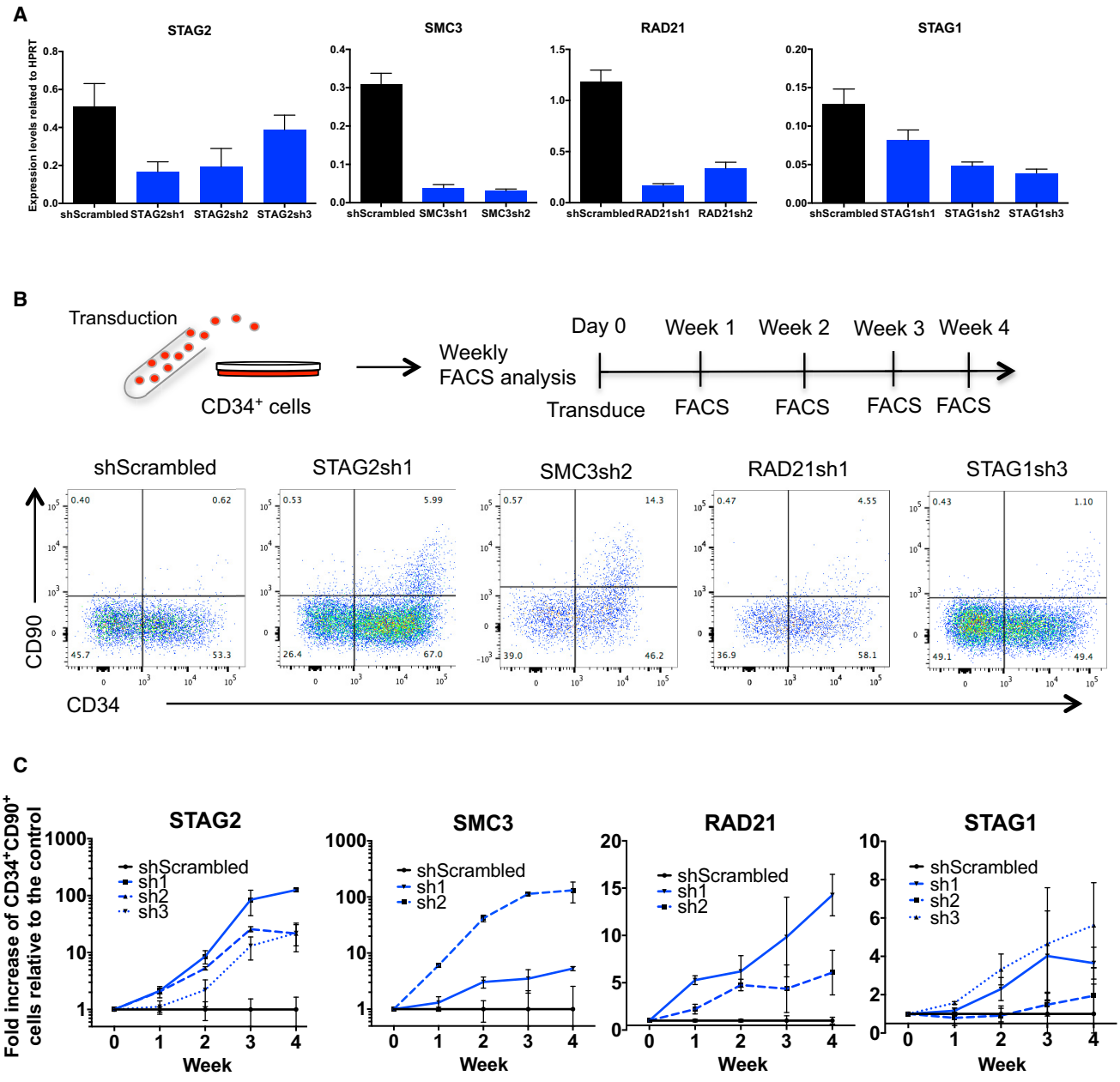

Figure 3. Knockdown of Cohesin Genes Impairs Differentiation and Expands Primitive Cells Ex Vivo

$CD34^+$ cells were transduced with shRNAs targeting RAD21, STAG2, SMC3, and STAG1 using 2 or 3 shRNAs per gene. Transduced cells were analyzed for the level knockdown and functionally assayed in in vitro expansion cultures.

(A) Knockdown efficiency of shRNAs targeting cohesin genes as measured by qPCR. Error bars represent SD.

(B) Overview of the in vitro expansion assay and representative fluorescence-activated cell sorting (FACS) plots showing CD34 and CD90 expression after 2 weeks of culture.

(C) Expansion of the $CD34^+CD90^+$ cell number over a period of 4 weeks for all tested cohesin genes compared to controls. Error bars represent SD.

See also Figures S2–S4.

chimerism in peripheral blood (PB) after 8 weeks, we observed significantly lower engraftment levels for the STAG2 knockdown cells compared to controls, while at 16 weeks post-transplantation the engraftment levels were more or less equal in PB (Figure 4B). However, strikingly, when examining the bone marrow (BM) after 16 weeks, there was a more than 2-fold increase in human cells in the STAG2-deficient group (Figure 4B). This indicates a delayed differentiation of STAG2-deficient HSPCs in vivo with a relative expansion of immature cells over time. When analyzing the BM-engrafted human cells in more detail, we

observed a myeloid skewing as determined by an increased fraction of CD33/15-positive cells for the STAG2-targeted cells (Figure 4C). Moreover these long-term engrafted cells displayed a significantly increased frequency of the HSC-enriched $CD34^+CD38^-$ population (Figure 4C), indicating an expansion at the level of HSCs as well. This increase of HSC numbers in vivo was functionally confirmed in secondary transplantation experiments in which the STAG2-deficient group, but not the control group, showed robust human engraftment levels (Figure 4D).

To verify that the observed in vivo phenotype was specifically associated with STAG2 knockdown but also relevant for other cohesin components, we performed similar transplantation experiment with an additional shRNA targeting STAG2, as well as two independent shRNAs targeting SMC3. Indeed, cells targeted by these other shRNAs showed significantly higher levels of human chimerism in the bone marrow of long-term engrafted animals (Figure 4E). The enhanced engraftment capability of cohesion-deficient HSCs was further strengthened in secondary transplants for shSMC3-transduced cells (Figure S5C). However, there were some notable differences between STAG2- and SMC3-targeted cells in terms of engraftment kinetics and differentiation patterns. First, engraftment levels in peripheral blood were higher in SMC3-targeted cells at 16 weeks, indicating a less severe impact on differentiation (Figure S5A). Moreover, both shRNAs for STAG2 triggered a pronounced myeloid skewing, while the two SMC3 shRNAs showed a normal myeloid/lymphoid distribution compared to control (Figure S5B). These differences in differentiation potential could either be due to distinct functions of SMC3 and STAG2, respectively, or a dosage effect at the level of the entire cohesin complex, where their respective knockdown from these particular shRNAs impairs the complex to a different extent.

Overall, our findings in vivo indicate a maturation block in cohesion-deficient HSCs resulting in delayed differentiation coupled with enhanced renewal and reconstitution potential. Several of the observed effects include features that are associated with myeloid neoplasms. However, we did not observe any signs of malignant disease in either primary or secondary transplanted mice for any of the STAG2/SMC3 shRNAs, indicating that cohesin deficiency alone may not be sufficient to trigger leukemia.

Silencing of Cohesin Genes Results in Immediate Transcriptional Changes with a Shift toward a More HSC-like Gene Expression Signature

The ring-like structure formed by the cohesin complex functions to hold chromatin strands together and was originally identified as a regulator of proper sister chromatid segregation during mitosis. Other functions of cohesin have recently been described, including control of DNA damage repair, as well as regulation of gene expression through mediation of long-range DNA interactions and accessibility to gene regulatory elements (Panigrahi and Pati, 2012).

To gain a basic understanding of the mechanisms behind the observed effects from cohesin knockdown, we performed transcriptome analysis of cohesin deficient cells. $CD34^+$ cells were transduced with shRNAs targeting each of the four cohesin genes in five independent replicates, and 36 hr later the cells were harvested and subjected to global gene expression profiling using microarrays (Figure 5A). We decided to minimize the time between transduction and transcriptome analysis in order to assess the immediate transcriptional changes triggered by cohesin knockdown independent of any secondary effects. Hierarchical clustering by Pearson correlation showed that all 20 cohesin knockdown samples clustered tightly together and were distinctly separated from three independent groups of control samples (Figure 5B). Next, we matched our expression dataset to a gene set specific for cord blood-derived HSCs (Laurenti et al., 2013) using gene set enrichment analysis (GSEA) software (Subramanian et al., 2005), and found that upregulated genes had a strong enrichment of HSC-specific genes, both when analyzing the knockdown of individual cohesin components (Figure S6A) and when analyzing all the components together (Figure 5C). The leading edge genes from this analysis are listed in Table S4. To validate the microarray data, we selected the top two genes of the HSC-specific leading edge (*CRHBP* and *MYCT1*) and two additional genes with a more established role in human HSCs (*SOCS2* and *KLF5*) and performed expression analysis by qPCR (Vitali et al., 2015; Taniguchi Ishikawa et al., 2013). We found the qPCR results to be similar to the microarray data (Figure S6B). Gene sets associated with cell cycle and apoptosis did not show any enrichment among the differentially expressed genes, suggesting that the immediate molecular consequences of cohesin deficiency are associated with a preserved immature state of the HSPCs rather than a proliferative response (Figure S6A). Our findings support a model in which the functional outcome of cohesin knockdown in HSPCs is triggered directly through alterations in its ability to control accessibility to transcriptional regulators, rather than secondary genetic events triggered by, for example, genomic instability from impaired sister chromatid separation or deficient DNA repair mechanisms.

DISCUSSION

We report here on the successful development of a genome-wide RNAi screening approach targeted to primary human hematopoietic stem and progenitor cells to define genes and pathways associated with self-renewal and differentiation. Based on findings from the screen, we implicate the cohesin complex as a crucial regulator of cell-fate decisions influencing self- renewal and differentiation in HSCs both in vitro and in vivo.

These efforts represent a genome-wide RNAi screen targeted to primary human HSPCs. The main limiting factor when performing functional screens in primary human cells is cell number. This obviously becomes even more challenging when rare cell subsets, such as stem and progenitor cells, are studied. Through unique access to cord blood with daily deliveries from several local hospitals, we were able to gather the necessary quantities to perform a screen in enriched primary HSPCs with reasonable coverage (300X). Overall, for the primary and secondary screens performed here, we isolated cells from more than 150 cord blood units. Despite access to these large quantities of cord blood, we reasoned that a screen in the most enriched HSC fraction would not yield sufficient coverage for a genome-wide library. We therefore used the assumption that pre-selecting genes

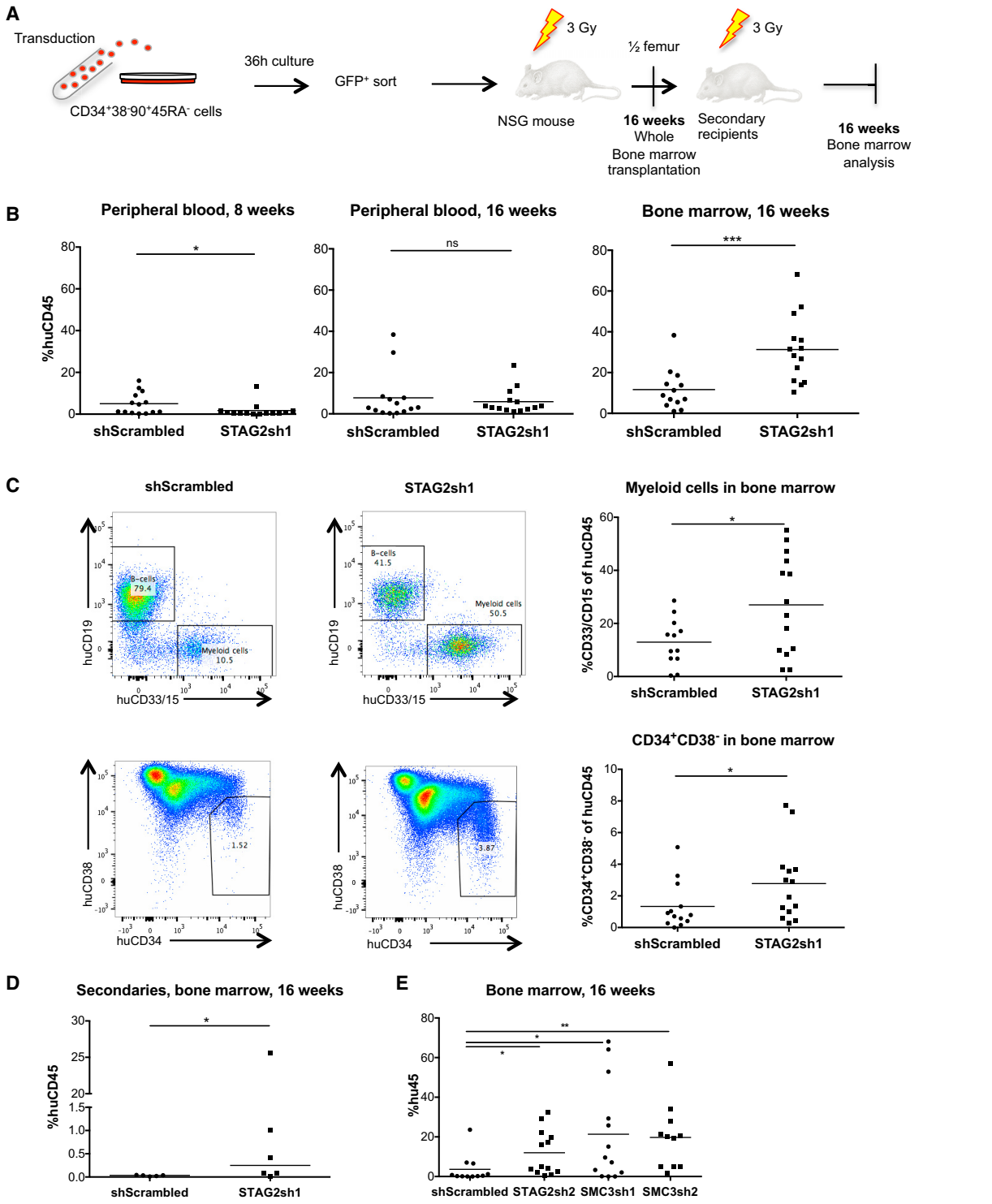

Figure 4. Cohesin-Deficient HSCs Show Increased Reconstitution Potential following Transplantation to Primary and Secondary Immunodeficient Mice

$CD34^+38^-90^+45RA^-$ cells were transduced with shRNAs targeting cohesin genes and assayed in vivo by transplantation to NSG mice.

(A) Overview of the in vivo transplantation assay for cohesion-deficient cells.

(B) Human chimerism in mice transplanted with shSTAG2-transduced cells as analyzed in peripheral blood after 8 and 16 weeks, and in bone marrow after 16 weeks.

(legend continued on next page)

influencing expansion in a broader population of HSPCs through a primary near genome-wide screen and then subsequently narrowing down potential candidates in a secondary screen using a more stringent assay and a better defined HSC target population ($CD34^+CD38^-CD90^+CD45RA^-$ cells) would allow us to identify genes specifically influencing HSC-fate options associated with self-renewal and differentiation, independent of any general effects on proliferation. It is clear from our further analysis of the cohesin genes that the approach successfully selected for relevant outcomes in that respect. Importantly, this two-step paradigm to globally screen for modifiers of HSC fate and many of the principles used for analysis are not limited to RNAi libraries but can be employed in a similar way with, e.g., CRISPR/Cas systems delivered through lentiviral vectors.

One of the biggest challenges when performing large-scale RNAi screens is to avoid false-positive hits triggered by off-target activity or, when using lentiviral delivery, positional effects from vector integration. These challenges were possible to address to some extent by ensuring that multiple shRNAs targeting a certain gene were identified and scored across many transduction replicates in the screen. Moreover, we added stringent parameters based on documented knockdown efficiency of the shRNAs, as well as relevant gene expression within the hematopoietic system to enhance the specificity and further avoid false-positive hits. Finally, we considered the expansion phenotype to be less influenced by aberrant toxicity or off-target activity compared to depletion events and therefore focused our analysis on the identification of negative regulators from the enriched fraction of shRNAs. These efforts of excluding false-positive results have inevitably filtered out a number of "true" hits, and the screen should therefore, for these reasons, not be regarded as a comprehensive assessment of all genes in the library. Nevertheless, our findings suggest that we were able to broadly define relevant candidates, both in terms of general expansion of $CD34^+$ cells and, more specifically, as mediators of self-renewal and differentiation in HSCs. The data from the screens presented here should therefore be a useful resource, providing candidate regulators of primary human HSPCs. As such our data may become useful to identify targets for ex vivo HSC expansion in cell-therapy applications, but also to better understand the molecular and genetic basis underlying malignant hematopoiesis.

Our first analysis of the primary screen showed a strong enrichment of cancer-related genes among the broadly defined candidate genes. This was a quite expected finding given that the selection was based on expansion of undifferentiated cells. The cohesin complex is also highly associated with cancer and during the last couple of years several studies have pointed to perturbed functions of cohesin in hematological malignancies. The prevalence of mutations in cohesin genes has been particularly striking, in acute myeloid leukemia (AML), where 12% of patients were reported to have mutations (Kon et al., 2013), as well as in myelodysplastic syndrome (MDS), where one study reports mutations in as many as 15% of patients (Leeke et al., 2014). Genome sequencing studies have revealed three particular characteristics about mutations in cohesin genes in AML and MDS patients, all of which can be reflected in our functional studies of cohesin deficiency in normal hematopoietic precursors. First, the mutations are often of inactivating character with a high allelic frequency, suggesting a tumor-suppressor function for cohesin with mutations acting as an early driver of events during leukemogenesis. Our functional studies showing increased renewal and impaired differentiation of HSPCs upon cohesin deficiency clearly support a strong tumor-suppressor role for cohesin. Second, cohesin mutations affect all gene members of the complex but do not co-occur suggesting that they are mutually exclusive (Welch et al., 2012). Our findings support this notion, as targeting several of the cohesin genes independently resulted in similar functional outcomes. Third, cohesin mutations are associated with an intact karyotype of the malignant cells, speaking against perturbation of the classical function of cohesin in regulating sister chromatid segregation as a major cause of malignant development. Rather, it has been suggested that the more recently defined role of cohesin in regulation of gene expression by mediating DNA accessibility to gene regulatory elements would be important in this context (Kagey et al., 2010). Our results provide support for this as cohesin knockdown triggered immediate transcriptional changes (upregulation of HSC specific genes) that could be linked to the functional outcome. These correlations between our cohesin-deficient HSPCs and hematopoietic malignancies with cohesin mutations illustrate the power of RNAi for functional modeling of haploinsufficient tumor suppressor genes whose incomplete loss of expression accelerates tumor development. A complete gene knockout strategy is not feasible in this context. For example, a complete disruption of cohesin is detrimental to cell survival and function (Rollins et al., 2004; Vass et al., 2003) and would not allow the identification of its role as a tumor suppressor. Haploinsufficient tumor suppressor genes are further particularly challenging to identify using standard genomic approaches as they can be affected by large heterozygous deletions that encompass many genes. Our identification of the cohesin genes illustrate how global RNAi screens in human HSPCs can complement genome sequencing approaches for the identification of functionally relevant tumor suppressor genes in hematopoietic malignancies.

While this paper was being prepared for submission, three other studies were published that reported on the functional role of cohesin in both murine and human hematopoiesis (Mazumbar et al., 2015; Mullenders et al., 2015; Viny et al., 2015). Two of these reports investigated mouse hematopoiesis using

(C) Myeloid and lymphoid engraftment measured by expression of CD15/CD33 and CD19, respectively, as well as levels of HSC engraftment ($CD34^+38^-$ cells) was measured in bone marrow 16 weeks after transplantation. Representative FACS plots gated on huCD45-positive cells, and the accumulated data are shown.
(D) Bone marrow cells from engrafted mice were transplanted to secondary recipient mice, and levels of human engraftment were measured again after 16 weeks for shSTAG2 and control transduced cells.
(E) Human chimerism in the bone marrow 16 weeks after primary transplantation of cells transduced with an additional shRNA targeting STAG2, as well as two shRNAs targeting SMC3. * $p < 0.05$, ** $p < 0.01$, *** $p < 0.001$.
See also Figure S5.

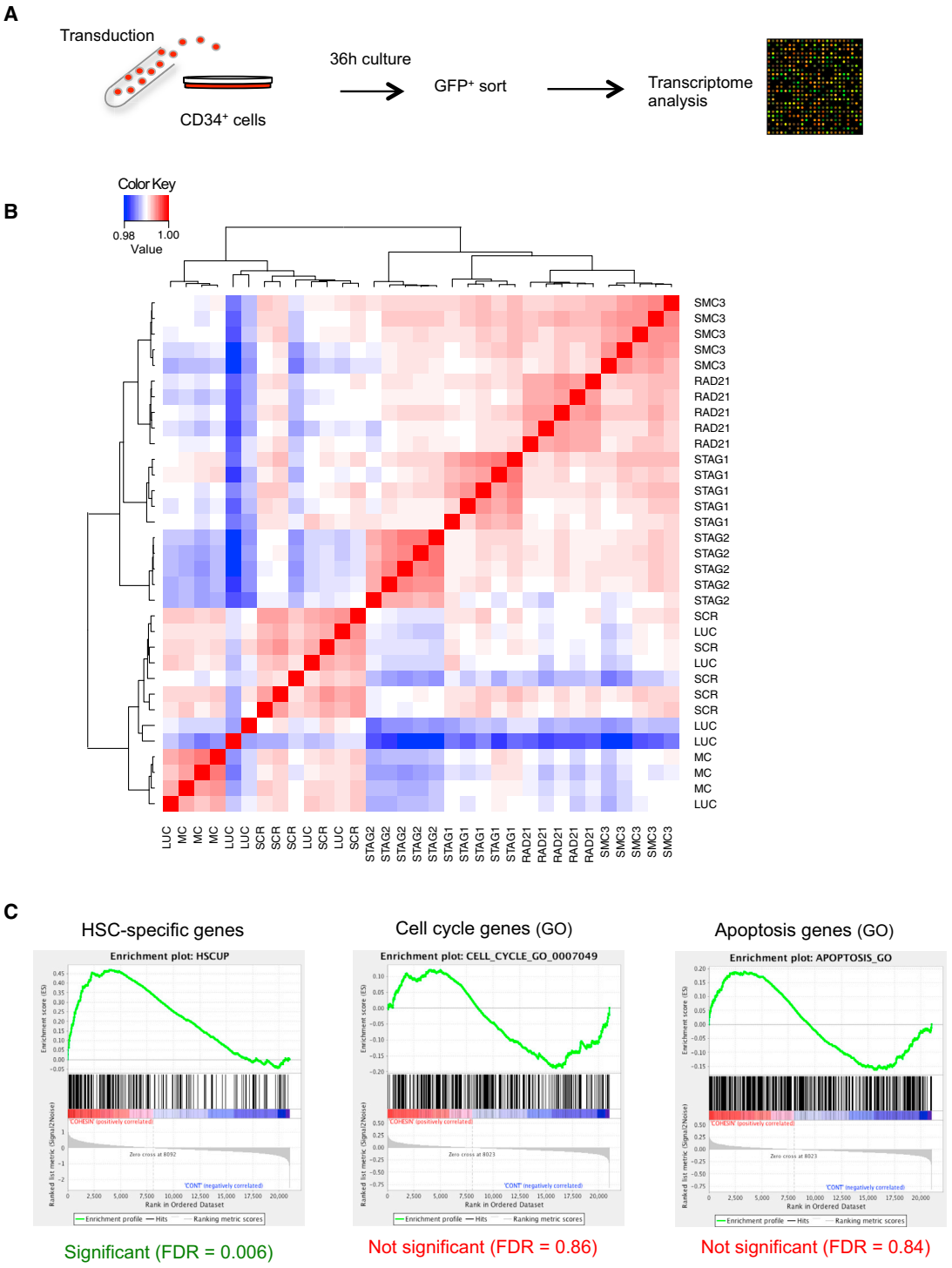

Figure 5. Silencing of Cohesin Genes Results in Immediate Transcriptional Changes with a Shift toward a More HSC-like Gene Expression Signature

(A) Outline of the transcriptional profiling experiment. CD34$^+$ cells were transduced with shRNAs targeting several cohesin genes, and transduced cells were subjected to transcriptome analysis on microarrays 36 hr after transduction.

(B) The data were subjected to unsupervised hierarchical clustering as illustrated in the Pearson correlation dendrogram.

(C) Gene set enrichment analysis (GSEA) to identify gene sets enriched in cohesin knockdown cells compared to controls. Plots using a gene set specific for HSCs (left), cell-cycle genes (middle), and apoptosis genes (right) are shown.

See also Figure S6 and Table S4.

either heterozygous knockout mice for *SMC3* (Viny et al., 2015) or shRNA knockdown for all the cohesin genes (Mullenders et al., 2015), and one study was performed in human cells by introducing mutant forms of the cohesin genes in $CD34^+$ cells to perturb the function of the complex (Mazumbar et al., 2015). Overall, the findings from these studies, as well as those from us, are remarkably consistent, given the profoundly different strategies used to perturb cohesin and the fact the studies have been performed in two different species. Nevertheless, all four reports convey a common theme of preservation of the immature phenotype of HSPCs, delayed or impaired differentiation potential, in many cases coupled with a skewing toward the myeloid lineage, as well as deregulated gene expression patterns commonly associated with a preserved HSC phenotype and reduced activation of lineage-specific gene programs. In our study, SMC3 knockdown cells showed increased engraftment levels in vivo, but in contrast to STAG2 knockdown, they did not display a marked differentiation block or myeloid skewing in vivo, despite a clear increase in undifferentiated cells in vitro. This was consistent for both SMC3 shRNAs tested and could indicate distinct roles for the different cohesin genes in regulation of HSPCs. However, the study by Viny et al. (2015) showed that transplantation of bone marrow from *Smc3* heterozygous knockout mice resulted in enhanced engraftment levels with a myeloid bias, consistent with our finding for STAG2, as well as the observations for RAD21 and Smc1a from the studies by Mazumbar et al. (2015) and Mullenders et al. (2015). This, together with the tightly clustered expression profiles upon knockdown of the cohesin genes, would argue against distinct roles of the different genes in the context of HSPC function. On the other hand, individual cohesin components may be differentially required within the complex, and their perturbation may therefore disrupt cohesin function to different extents. This is supported by the varying prevalence of mutations for the cohesin genes in myeloid neoplasms, with *STAG2* and *RAD21* mutations being most common. It is possible that the SMC3 knockdown in our setting was not sufficient to induce myeloid skewing in the NSG transplantation model, which is heavily biased toward lymphoid reconstitution from human cells and normally shows very low levels of myeloid cells.

Taken together, these four recent studies strongly point toward a highly specific and dominant role of cohesin in regulating cell-fate decisions in HSCs. Moreover, they provide a solid functional basis to understand the involvement of cohesion deficiency in myeloid malignancies. Mechanistically, all these studies point toward alterations in *cis*-regulatory chromatin architecture affecting gene transcription as the primary driver of the cohesin-deficient phenotypes. However, the precise details of how this occurs and which genes that may be critical targets in the context of HSC function remains to be defined. Our gene expression profiling identified a number of HSC-associated genes, several of which have defined functions in HSC regulation, such as *ERG*, *EGR1*, *KLF5*, and *SOCS2*, and it is possible that one or more of these could be mediating the phenotype observed upon cohesin disruption (Knudsen et al., 2015; Min et al., 2008; Vitali et al., 2015; Taniguchi Ishikawa et al., 2013). Overall, it is indeed an intriguing concept for further exploration that perturbations in a generic complex like cohesin, with essential functions in all dividing cells, can result in the activation of coordinated gene programs in stem cells.

EXPERIMENTAL PROCEDURES

Primary Human Samples

Human cord blood (CB) samples were obtained from the maternity wards of Helsingborg General Hospital and Skåne University Hospital in Lund and Malmö, Sweden, after informed, written consent according to guidelines approved by the regional ethical committee. Samples were only collected from uncomplicated births, and no samples older than 24 hr were used. Mononuclear cells were separated through density-gradient centrifugation (Lymphoprep, #1019818A, Medinor). $CD34^+$ cells were magnetically isolated (#189-046703, Fisher Scientific).

Primary Screen

$CD34^+$ cells were lentivirally transduced with a pooled, genome-wide shRNA library (#SHPH01, Sigma-Aldrich) as previously described (Baudet et al., 2012) and subsequently passaged in serum-free expansion medium (SFEM, Stem Cell Technologies), supplemented with stem cell factor (SCF), thrombopoietin (TPO), and FLT3-ligand (FLT3L) at 100 ng/ml from Peprotech (hereafter abbreviated as STF). Genomic DNA from cells was collected at day 3 and at day 20 after magnetic CD34 enrichment and isolated with the High Pure PCR Template Preparation Kit (#11796828001, Roche Diagnostics). Provirus integration sites were PCR amplified in 5% DMSO with 1 M Betaine (Figure S1C) and sequenced on the Illumina Genome Analyzer II.

Gene Ontology and KEGG Pathway Analysis

To identify genes from the primary screen for preliminary analysis, shRNAs represented in less than three replicates were removed. Each shRNA was then scored based on its mean enrichment value across all replicates in the primary screen. Genes with at least two shRNA among the top 10% were selected. Gene ontology analysis was conducted using the Panther overrepresentation test with Bonferroni correction with a cutoff of $p < 0.05$. KEGG analysis was used to study pathways, using same settings as for gene ontology.

Secondary Screen

350 shRNAs targeting the highest scoring 150 genes were used to transduce sorted $CD34^+38^-90^+45RA^-$ cells. 10 days after culture, cells were stained for CD34 and CD90 and sorted for three distinct populations: $CD34^+CD90^+$, $CD34^+CD90^-$, and $CD34^-CD90^-$. Cells were processed as described above.

Lentiviral Production

Lentiviruses were produced in the human 293T cell line as previously described (Ali et al., 2009).

Gene Expression

Levels of gene expression and knockdown were ascertained with qPCR probes from Taqman, Life Technologies: HPRT1 (Hs02800695_m1), (STAG2 (Hs00198227_m1), RAD21 (Hs00366721_mH), SMC3 (Hs00271322_m1), STAG1 (Hs00195307_m1), MYCT1 (Hs00228305_m1), CRHBP (Hs00181810_m1), SOCS2 (Hs00919620_m1), KLF5 (Hs00156145_m1). 36 hr post-transduction, sorted GFP^+ cells were processed using the manufacturer's instructions (RNeasy #74004, QIAGEN). Superscript III (#18080085, Life Technologies) was used for reverse transcription. mRNA levels were normalized to HPRT.

In Vitro Culture

Transduced CB-derived $CD34^+$ cells were cultured in in SFEM/STF and stained in PBS/2% fetal calf serum (FCS) for CD34 and CD90 expression every week. Viability stain was done with 7-Aminoactinomycin D, (Sigma-Aldrich, #A-9400).

Human Engraftment Assay

Sorted $CD34^+38^-90^+45RA^-$ cells at the equivalent of 50,000 transduced $CD34^+$ cells were intravenously injected into the tail vein of sublethally (3 Gy)

irradiated NOD.Cg-Prkdc^{scid}Il2rg^{tm1Wjl}/SzJ (NSG) mice. Human chimerism was assayed in the peripheral blood (tail vein sampling) after 8 weeks and from peripheral blood, bone marrow (left and right tibia, femur, and iliac bones), and spleen after 16 weeks. All animal experiments were approved by the Lund/Malmö Ethical Committee for Animal Research.

Microarray Analysis

Transduced CB-derived CD34$^+$ cells were cultured in in SFEM/STF for 36 hr. GFP$^+$ cells were sorted and analyzed using the Human Genome U133$^+$ array. For details, please see the Supplemental Experimental Procedures.

Statistical Analysis

Statistical significance was calculated in GraphPad Prism (v.6.0) using paired Student's t test. Error bars represent SD unless indicated otherwise.

ACCESSION NUMBERS

The accession number for the microarray data reported in this paper has been uploaded to GEO: GSE74824.

SUPPLEMENTAL INFORMATION

Supplemental Information includes Supplemental Experimental Procedures, six figures, and four tables and can be found with this article online at http://dx.doi.org/10.1016/j.celrep.2016.02.082.

AUTHOR CONTRIBUTIONS

R.G. and J.L. conceived of the study and designed the experiments. R.G., A.B., P.K., A.R.N., and T.T. performed the experiments. R.G., B.N., S.S., and A.K. analyzed the data. Å.B. and J.L. provided resources. R.G. and J.L. wrote the paper.

ACKNOWLEDGMENTS

The authors would like to thank Mats Bergstrand, Beata Lindkvist, Karin Olsson, Ineke de Jong, and Carolina Guibentif for assistance with the experiments and analysis. This work was funded by grants from the Swedish Research Council, the Swedish Cancer Foundation, and the Swedish Pediatric Cancer Foundation. This project has also received funding from the European Research Council under the European Union's Horizon 2020 research and innovation program (grant agreement no. 648894) (to J.L.). The work was also supported by the HematoLinné and StemTherapy programs at Lund University.

Received: November 24, 2015
Revised: February 4, 2016
Accepted: February 22, 2016
Published: March 17, 2016

REFERENCES

Ali, N., Karlsson, C., Aspling, M., Hu, G., Hacohen, N., Scadden, D.T., and Larsson, J. (2009). Forward RNAi screens in primary human hematopoietic stem/progenitor cells. Blood *113*, 3690–3695.

Baudet, A., Karlsson, C., Safaee Talkhoncheh, M., Galeev, R., Magnusson, M., and Larsson, J. (2012). RNAi screen identifies MAPK14 as a druggable suppressor of human hematopoietic stem cell expansion. Blood *119*, 6255–6258.

Cellot, S., Hope, K.J., Chagraoui, J., Sauvageau, M., Deneault, É., MacRae, T., Mayotte, N., Wilhelm, B.T., Landry, J.R., Ting, S.B., et al. (2013). RNAi screen identifies Jarid1b as a major regulator of mouse HSC activity. Blood *122*, 1545–1555.

Chou, S., Chu, P., Hwang, W., and Lodish, H. (2010). Expansion of human cord blood hematopoietic stem cells for transplantation. Cell Stem Cell *7*, 427–428.

Dahlberg, A., Delaney, C., and Bernstein, I.D. (2011). Ex vivo expansion of human hematopoietic stem and progenitor cells. Blood *117*, 6083–6090.

Gruber, S., Haering, C.H., and Nasmyth, K. (2003). Chromosomal cohesin forms a ring. Cell *112*, 765–777.

Hannon, G.J., and Rossi, J.J. (2004). Unlocking the potential of the human genome with RNA interference. Nature *431*, 371–378.

Hope, K.J., Cellot, S., Ting, S.B., MacRae, T., Mayotte, N., Iscove, N.N., and Sauvageau, G. (2010). An RNAi screen identifies Msi2 and Prox1 as having opposite roles in the regulation of hematopoietic stem cell activity. Cell Stem Cell *7*, 101–113.

Kagey, M.H., Newman, J.J., Bilodeau, S., Zhan, Y., Orlando, D.A., van Berkum, N.L., Ebmeier, C.C., Goossens, J., Rahl, P.B., Levine, S.S., et al. (2010). Mediator and cohesin connect gene expression and chromatin architecture. Nature *467*, 430–435.

Karlsson, C., Rak, J., and Larsson, J. (2014). RNA interference screening to detect targetable molecules in hematopoietic stem cells. Curr. Opin. Hematol. *21*, 283–288.

Kinkel, S.A., Galeev, R., Flensburg, C., Keniry, A., Breslin, K., Gilan, O., Lee, S., Liu, J., Chen, K., Gearing, L.J., et al. (2015). Jarid2 regulates hematopoietic stem cell function by acting with polycomb repressive complex 2. Blood *125*, 1890–1900.

Knudsen, K.J., Rehn, M., Hasemann, M.S., Rapin, N., Bagger, F.O., Ohlsson, E., Willer, A., Frank, A.K., Søndergaard, E., Jendholm, J., et al. (2015). ERG promotes the maintenance of hematopoietic stem cells by restricting their differentiation. Genes Dev. *29*, 1915–1929.

Kon, A., Shih, L.Y., Minamino, M., Sanada, M., Shiraishi, Y., Nagata, Y., Yoshida, K., Okuno, Y., Bando, M., Nakato, R., et al. (2013). Recurrent mutations in multiple components of the cohesin complex in myeloid neoplasms. Nat. Genet. *45*, 1232–1237.

Laurenti, E., Doulatov, S., Zandi, S., Plumb, I., Chen, J., April, C., Fan, J.B., and Dick, J.E. (2013). The transcriptional architecture of early human hematopoiesis identifies multilevel control of lymphoid commitment. Nat. Immunol. *14*, 756–763.

Leeke, B., Marsman, J., O'Sullivan, J.M., and Horsfield, J.A. (2014). Cohesin mutations in myeloid malignancies: underlying mechanisms. Exp. Hematol. Oncol. *3*, 13.

Majeti, R., Park, C.Y., and Weissman, I.L. (2007). Identification of a hierarchy of multipotent hematopoietic progenitors in human cord blood. Cell Stem Cell *1*, 635–645.

Mazumbar, C., Shen, Y., Xavy, S., Zhao, F., Reinisch, A., Li, R., Ryan Corces, M., Flynn, R.A., Buenrostro, J.D., Chan, S.M., et al. (2015). Leukemia-associated cohesin mutants dominantly enforce stem cell programs and impair human hematopoietic progenitor differentiation. Cell Stem Cell *17*, 675–688.

Miller, P.G., Al-Shahrour, F., Hartwell, K.A., Chu, L.P., Järås, M., Puram, R.V., Puissant, A., Callahan, K.P., Ashton, J., McConkey, M.E., et al. (2013). In vivo RNAi screening identifies a leukemia-specific dependence on integrin beta 3 signaling. Cancer Cell *24*, 45–58.

Min, I.M., Pietramaggiori, G., Kim, F.S., Passegué, E., Stevenson, K.E., and Wagers, A.J. (2008). The transcription factor EGR1 controls both the proliferation and localization of hematopoietic stem cells. Cell Stem Cell *2*, 380–391.

Mullenders, J., Aranda-Orgilles, B., Lhoumaud, P., Keller, M., Pae, J., Wang, K., Kayembe, C., Rocha, P.P., Raviram, R., Gong, Y., et al. (2015). Cohesin loss alters adult hematopoietic stem cell homeostasis, leading to myeloproliferative neoplasms. J. Exp. Med. *212*, 1833–1850.

Nasmyth, K., and Haering, C.H. (2009). Cohesin: its roles and mechanisms. Annu. Rev. Genet. *43*, 525–558.

Orkin, S.H., and Zon, L.I. (2008). Hematopoiesis: an evolving paradigm for stem cell biology. Cell *132*, 631–644.

Panigrahi, A.K., and Pati, D. (2012). Higher-order orchestration of hematopoiesis: is cohesin a new player? Exp. Hematol. *40*, 967–973.

Papaemmanuil, E., Gerstung, M., Malcovati, L., Tauro, S., Gundem, G., Van Loo, P., Yoon, C.J., Ellis, P., Wedge, D.C., Pellagatti, A., et al.; Chronic Myeloid Disorders Working Group of the International Cancer Genome Consortium (2013). Clinical and biological implications of driver mutations in myelodysplastic syndromes. Blood *122*, 3616–3627, quiz 3699.

Rollins, R.A., Korom, M., Aulner, N., Martens, A., and Dorsett, D. (2004). Drosophila nipped-B protein supports sister chromatid cohesion and opposes the stromalin/Scc3 cohesion factor to facilitate long-range activation of the cut gene. Mol. Cell. Biol. *24*, 3100–3111.

Subramanian, A., Tamayo, P., Mootha, V.K., Mukherjee, S., Ebert, B.L., Gillette, M.A., Paulovich, A., Pomeroy, S.L., Golub, T.R., Lander, E.S., and Mesirov, J.P. (2005). Gene set enrichment analysis: a knowledge-based approach for interpreting genome-wide expression profiles. Proc. Natl. Acad. Sci. USA *102*, 15545–15550.

Taniguchi Ishikawa, E., Chang, K.H., Nayak, R., Olsson, H.A., Ficker, A.M., Dunn, S.K., Madhu, M.N., Sengupta, A., Whitsett, J.A., Grimes, H.L., and Cancelas, J.A. (2013). Klf5 controls bone marrow homing of stem cells and progenitors through Rab5-mediated β1/β2-integrin trafficking. Nat. Commun. *4*, 1660.

Vass, S., Cotterill, S., Valdeolmillos, A.M., Barbero, J.L., Lin, E., Warren, W.D., and Heck, M.M. (2003). Depletion of Drad21/Scc1 in Drosophila cells leads to instability of the cohesin complex and disruption of mitotic progression. Curr. Biol. *13*, 208–218.

Viny, A.D., Ott, C.J., Spitzer, B., Rivas, M., Meydan, C., Papalexi, E., Yelin, D., Shank, K., Reyes, J., Chiu, A., et al. (2015). Dose-dependent role of the cohesin complex in normal and malignant hematopoiesis. J. Exp. Med. *212*, 1819–1832.

Vitali, C., Bassani, C., Chiodoni, C., Fellini, E., Guarnotta, C., Miotti, S., Sangaletti, S., Fuligni, F., De Cecco, L., Piccaluga, P.P., et al. (2015). SOCS2 controls proliferation and stemness of hematopoietic cells under stress conditions and its deregulation marks unfavorable acute leukemias. Cancer Res. *75*, 2387–2399.

Welch, J.S., Ley, T.J., Link, D.C., Miller, C.A., Larson, D.E., Koboldt, D.C., Wartman, L.D., Lamprecht, T.L., Liu, F., Xia, J., et al. (2012). The origin and evolution of mutations in acute myeloid leukemia. Cell *150*, 264–278.

Zuber, J., Shi, J., Wang, E., Rappaport, A.R., Herrmann, H., Sison, E.A., Magoon, D., Qi, J., Blatt, K., Wunderlich, M., et al. (2011). RNAi screen identifies Brd4 as a therapeutic target in acute myeloid leukaemia. Nature *478*, 524–528.